Supplementory Information

ZIF-8@$CoFe_2O_4$ as a highly efficient bifunctional electrocatalyst for methanol oxidation and oxygen evolution reactions

T. V. M. Sreekanth[a], K. Prasad[b], J. Yoo[c]*, J. Kim[b]*, K. Yoo[a]**

[a]School of Mechanical Engineering, Yeungnam University, 38541 Gyeongsan-si, Republic of Korea

[b]Energy Storage Conversion Laboratory, Department of Electrical Engineering,Chungnam National University, 34134 Daejeon, Republic of Korea

[c]Department of Automobile Engineering, Hanyang University, Seoul-04763, Republic of Korea

---

**Corresponding author: Prof. K. Yoo; Email: *kisooyoo@yu.ac.kr*

*Co-corresponding author: Prof. J. Yoo: jihyungyoo@hanyang.ac.kr

Prof. J. Kim; Email: *whdgns0422@cnu.ac.kr*

Chemical and Reagents

Zinc nitrate hexahydrate, 2-methylimidazole, cobalt iron oxide nanoparticles, and methanol were purchased from Sigma-Aldrich. All reagents were of analytical grade and used as received without further purification.

Characterization

The crystallinity of the as-prepared samples was measured using powder X-ray diffraction (XRD; PANalytical X'Pert PRO, USA) with a Cu Kα radiation source (λ = 1.5405 Å). Fourier-transform infrared (FTIR; Perkin-Elmer, Bruker) spectroscopy in attenuated total reflectance mode was performed to determine the vibrational modes of the samples. The elemental composition was determined by X-ray photoelectron spectroscopy (XPS; K-Alpha, Thermo Scientific, USA) using Al-Kα radiation (1486.6 eV). The morphologies of the samples were investigated via scanning electron microscopy with a field emission gun (S4800, Hitachi, Japan) and high-resolution transmission electron microscopy (HR-TEM; Tecnai G2 F20 S-TWIN, FEI, USA) with an emission field gun of 200 kV in Schottky mode. Energy-dispersive X-ray analysis of the samples was performed using an X-ray column attached to the TEM instrument. The surface areas of the electrocatalysts were determined using 3Flex (Micromeritics, Norcross, GA, USA).

Fabrication of working electrodes

A slurry was obtained by mixing the synthesized electrocatalyst (80 %), carbon black (10 %), and a poly (vinylidene fluoride) (PVDF-10 %) binder in NMP solvent. This slurry was coated onto a Ni foam current collector via drop casting. The coated current collector was dried for 10 h. The electrochemical cell with the electrode system consisted of a coated electrode as the working electrode, a Pt electrode as the counter electrode, and Hg/HgO as the reference electrode. The working electrode coated with the electrocatalyst was studied in alkaline (1.0 M KOH) and alcohol (1.0 M methanol) media.

Electrochemical Characterization

The electrocatalytic performance was analyzed using electrochemical techniques such as cyclic voltammetry (CV), linear sweep voltammetry (LSV), electrochemical impedance spectroscopy (EIS), and chronoamperometry (CA) in a three-electrode system using a KOH (alkaline medium) electrolyte with and without the addition of methanol. CV analysis was performed at different scan rates in the 20–120 mV s^{-1}. The methanolelectro–oxidation reaction was performed in the potential range 0–0.7 V. The LSV was measured in 0.0–1.0 V vs Hg/HgO at 5 mV s^{-1}. EIS analyses were performed in a frequency range between 100 mHz and 1.0 MHz. The stability of the prepared samples was studied by chronoamperometry for up to 6 h.

The activity of the electrocatalysts was determined using the ECSA values. To determine the ECSA values of the electrocatalysts, CV measurements were performed in the nonFaradaic region of 0.03–0.015 V vs. the Hg/HgO electrode. The ECSA was calculated using the following equation [1].

$$\text{ECSA} = \frac{C_{dl}}{C_s}, \quad \text{(s1)}$$

where C_{dl} is the double-layer capacitance. Studies have shown that the double-layer charging current of a given capacitor generally levels off when plotted against the scan rate. This line is linearly related to $C_{dl,}$ and the slope of the plot is equivalent to C_{dl}. Further, Cs is the general specific capacitance (0.04 mF cm^{-2}), as reported in previous studies [1, 2]

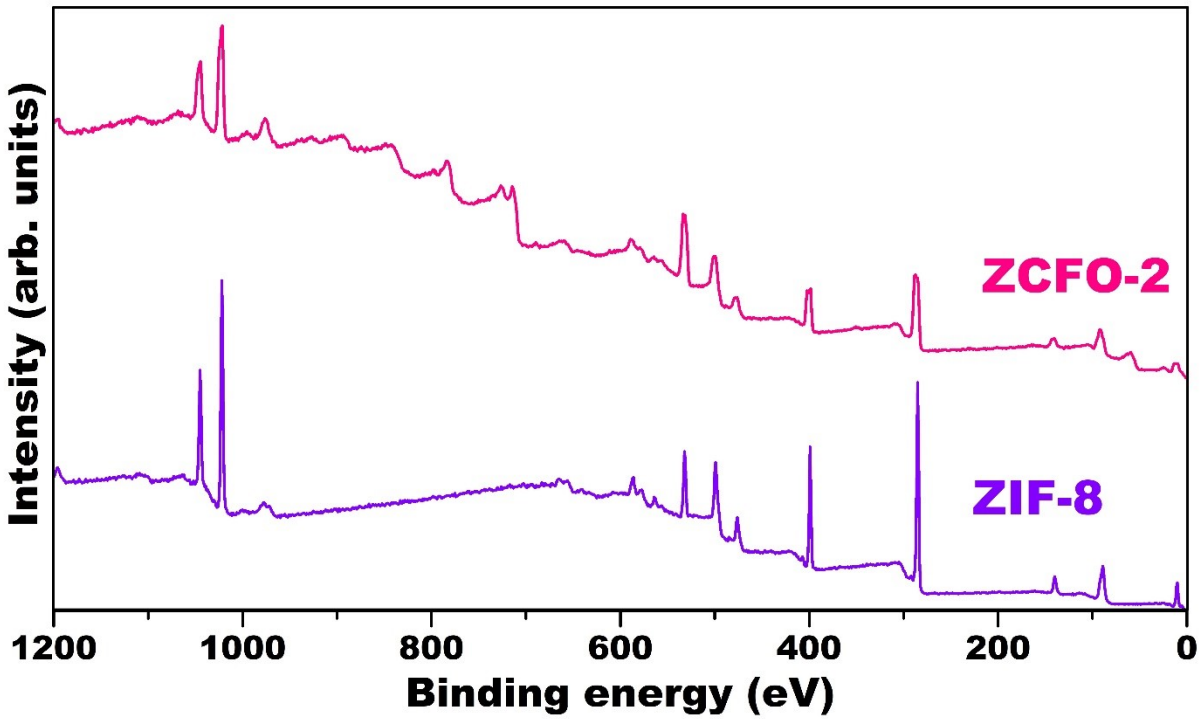

Fig. S1 Survey scan spectra of ZIF-8 and ZCFO-1 electrocatalysts.

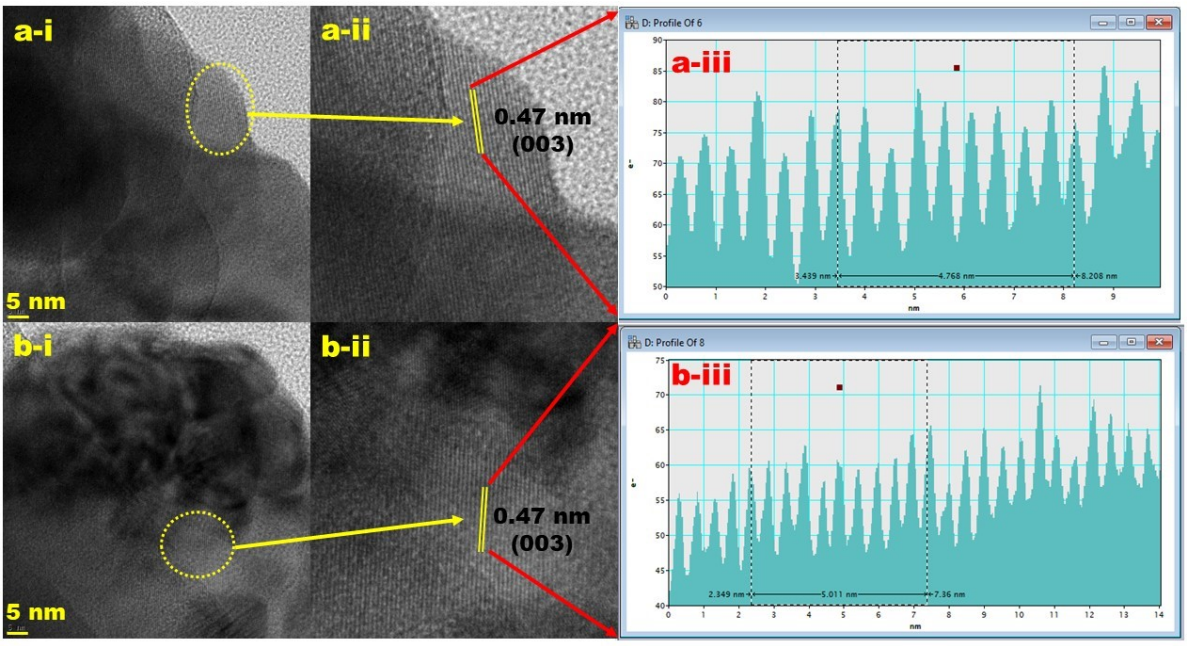

Fig. S2 (a-i), (b-ii) HR-TEM images, (a-ii), (b-ii) magnified TEM images along with d-spacing values, and (a-iii), (b-iii) corresponding line-profile images of the ZCFO-1 electrocatalyst.

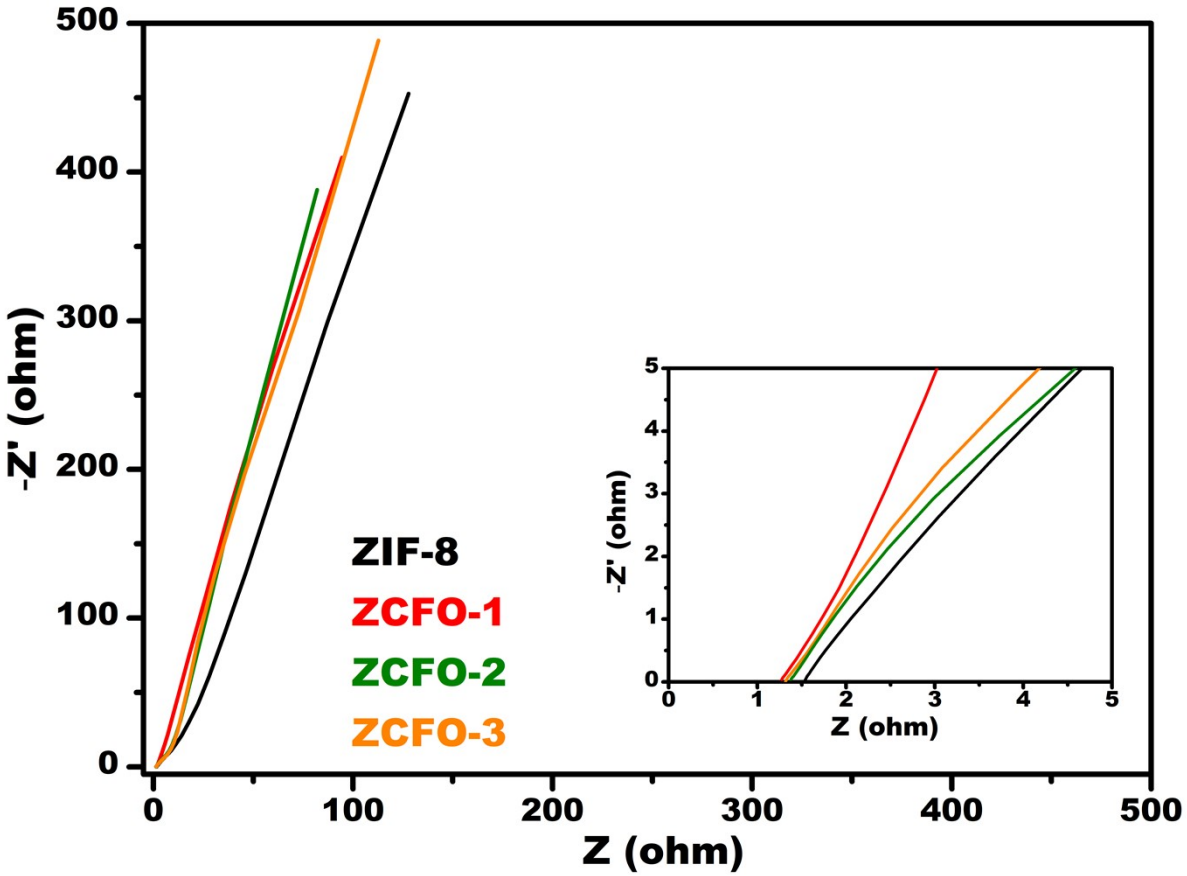

Fig. S3. Nyquist plots of the electrocatalysts ZIF-8, ZCFO-1, ZCFO-2, and ZCFO-3 (d) electrocatalysts in 1.0 M KOH.

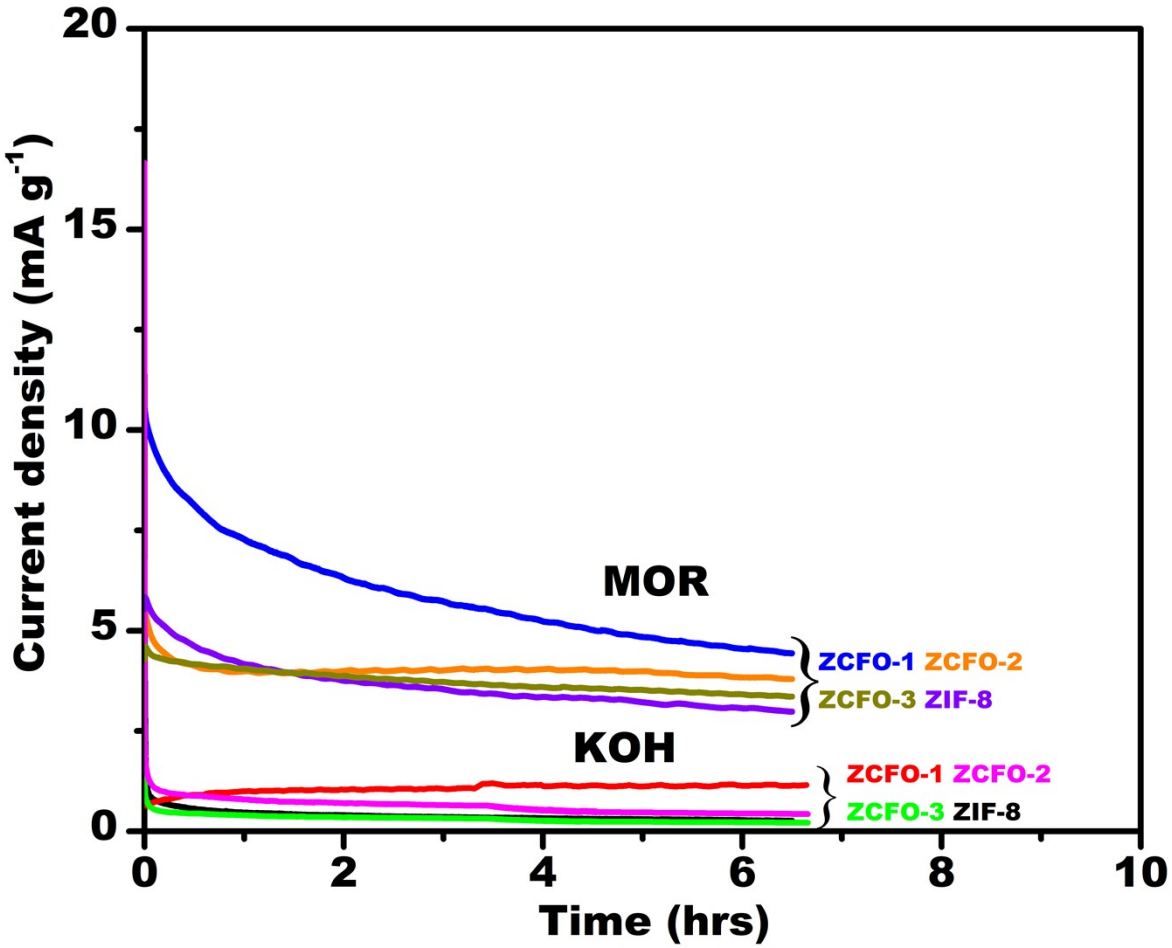

Fig. S4. Chronoamperometry curves of the ZIF-8, ZCFO-1, ZCFO-2, and ZCFO-3 (d) electrocatalysts in 1.0 M KOH along with 1.0 M of methanol

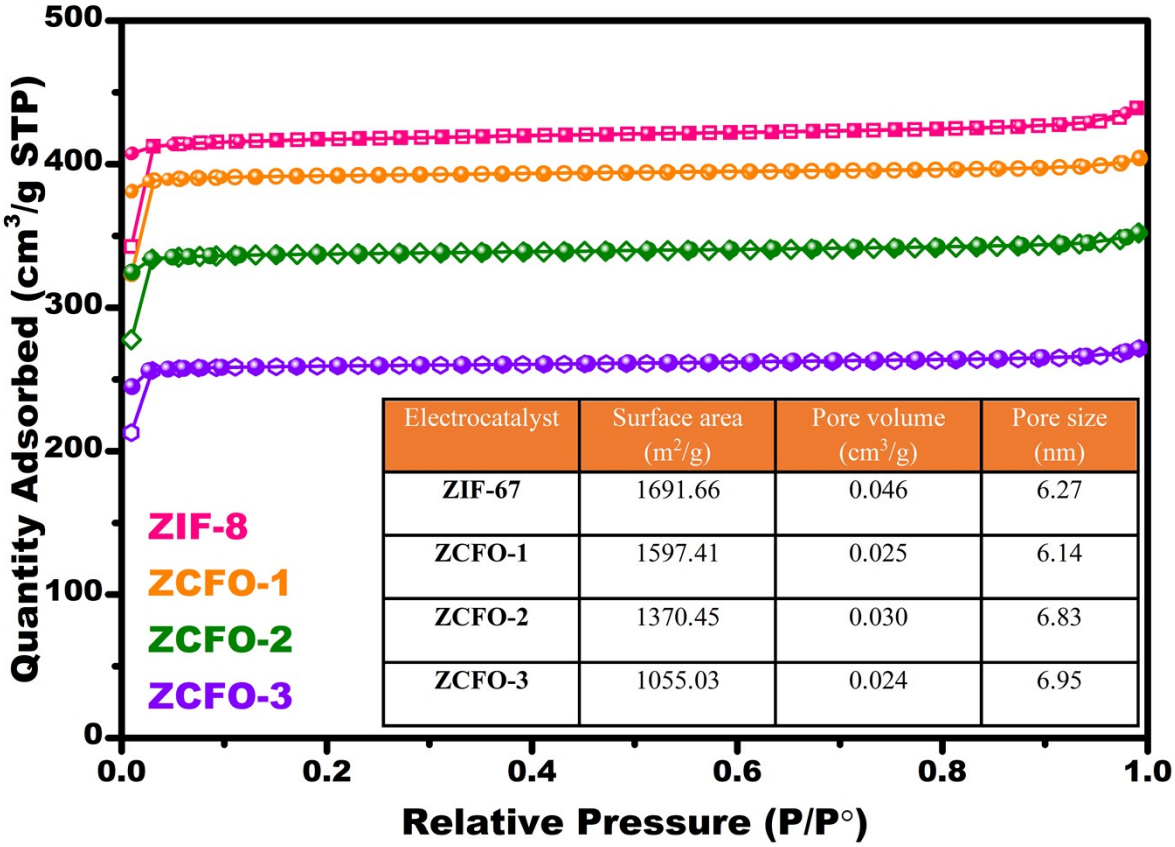

Fig. S5. Surface area analysis results: N_2 adsorption−desorption isotherm plots of (a) ZIF-8, (b) ZCFO-1, (c) ZCFO-2, and (d) ZCFO-3; Inset table represent the pore volume and pore size distribution results calculated from the BJH.

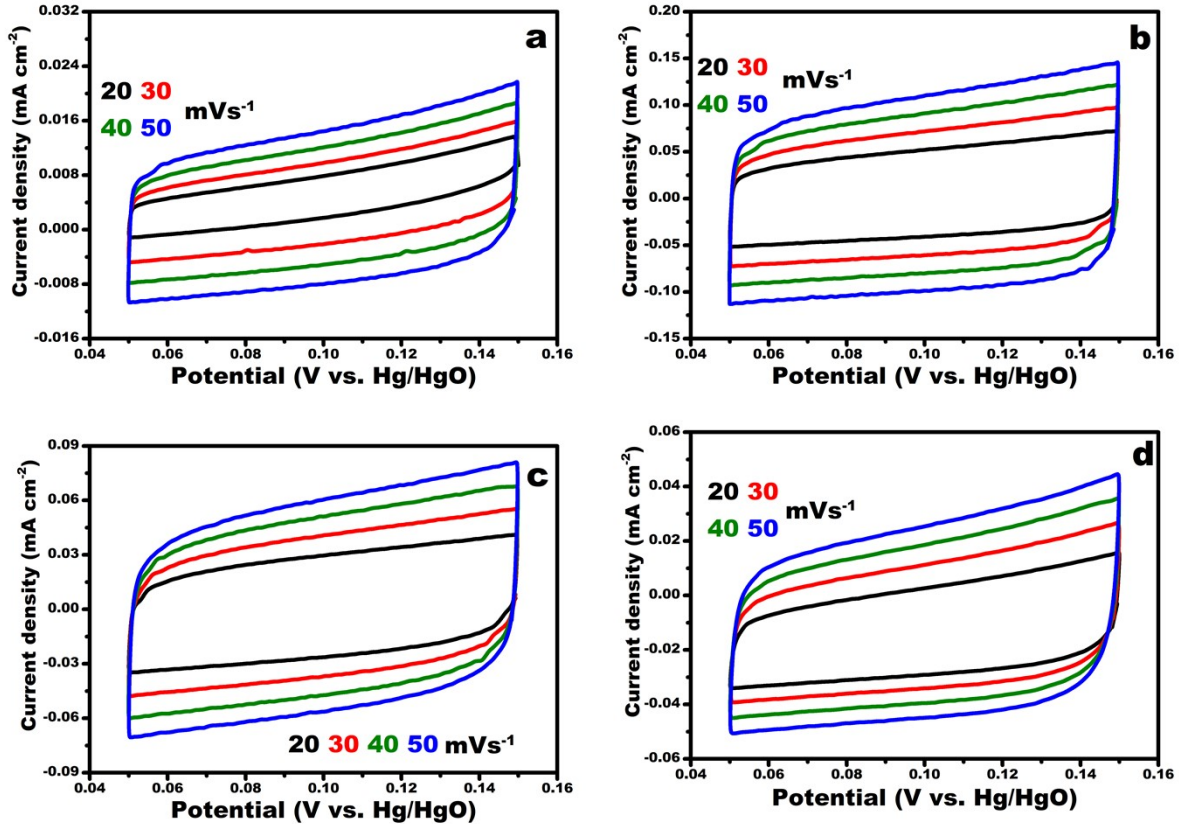

Fig. S6. CV curves of electrochemical active surface area test (ECSA) of (a) ZIF-8, (b) ZCFO-1, (c) ZCFO-2, and (d) ZCFO-3.

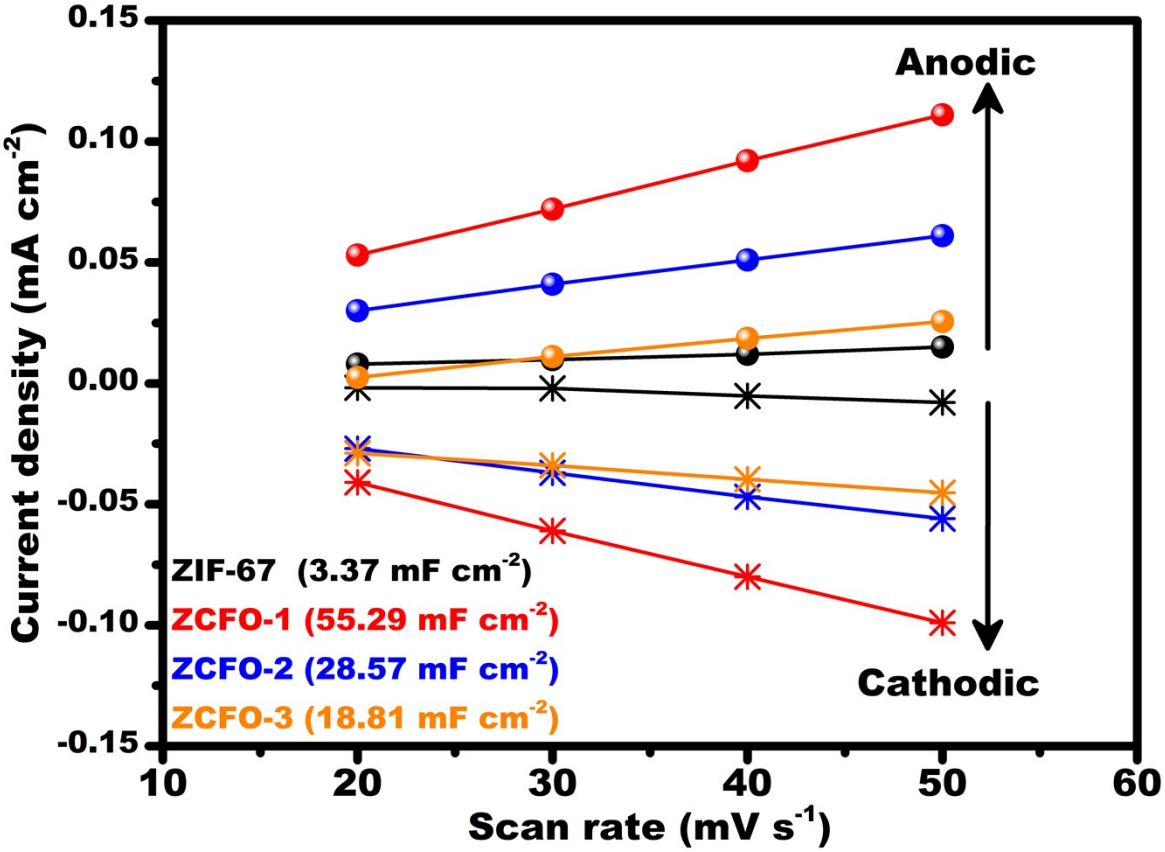

Fig. S7. Electrochemical double-layer capacity (C_{dl}) of electrocatalysts.

Table. S1 Comparison of MOFs based electrocatalysts in MOR analysis

Electrocatalyst	**Electrolyte**	**MOR activity Current/current denisty**	**Ref**
Ni- doped ZIF-8	0.1 M NaOH & 0.05 M MeOH	0.744 mA cm^{-2}	3-43
Ni- doped ZIF-67	0.1 M NaOH & 0.05 M MeOH	2.5 mA cm^{-2}	4-65
Ni- doped MIL-110	0.1 M NaOH & 0.1 M MeOH	14.4 mA cm^{-2}	5-80
Ni-MOF	0.5 M NaOH & 4.0 M MeOH	90 mA cm^{-2}	6-78
ZIF-8 thin film	0.5 M NaOH & 0.5 M MeOH	0.25 mA cm^{-2}	7-63
MoS_2@CoNi-ZIF	1.0 M KOH & 0.5 M MeOH	430.08 $mAcm^{-2}$	8-114
Ni/Zn-MOFs	0.1 M NaOH & 4.76 mM MeOH	300 μA	9-119
Ni-BTC/ 4wt% rGO	1.0 M NaOH & 2.0 M MeOH	200.2 $mAcm^{-2}$	10-77
ZIF-8	1.0 M KOH & 0.5 M MeOH	21.32 mA g^{-1}	Present work
ZCFO-1	1.0 M KOH & 0.5 M MeOH	40.84 mA g^{-1}	
ZCFO-2	1.0 M KOH & 0.5 M MeOH	29.72 mA g^{-1}	
ZCFO-3	1.0 M KOH & 0.5 M MeOH	24.83 mA g^{-1}	

Table. S2 Comparison of ZIF-8 and $CoFe_2O_4$ based electrocatalysts in OER analysis

Electrocatalyst	**Electrolyte**	**Overpotential (10 mA cm^{-2})**	**Tafel slope (mV dce^{-1})**	**Ref**
CFO	1.0 M KOH	360	115	11
CFO-Sn1	1.0 M KOH	320	88	
CFO-Sn2	1.0 M KOH	290	85	
$CoFe_2O_4$/NF	1.0 M KOH	273	102	12
$CoFe_2O_4$/biomass carbon hybrid	1.0 M NaOH	300	86	13
$CoFe_2O_4$/SWNTs	1.0 M KOH	310	85	14
Au-$CoFe_2O_4$	1.0 M KOH	312	46.8	15
$CoFe_2O_4$	1.0 M KOH	374	35	

$CoFe_2O_4$ Nanoplates	1.0 M NaOH	410	61	16
$CoFe_2O_4$/rGO	1.0 M KOH	340	31	17
Reduced CoFe2O4	1.0 M KOH	320	94	18
$CoFe_2O_4$ NPs	1.0 M KOH	450	48	
$CoFe_2O_4$-CoFex/C	1.0 M KOH	350	---	19
ZIF-67@POM	1.0 M KOH	287	58	20
ZIF-67@NPC-2 (2:1)	0.1 M KOH	410	114	21
CoO_x-ZIF	0.1 M NaOH	318	70.3	22
Co-ZIF-9	0.1 M KOH	510	93	23
ZIF-8@ZIF-67@POM	1.0 M KOH	490	88	24
SiW_9Co_3[h]@ZIF-67	0.1 M KOH	420	94	25
Fe/$Ni_{2.4}$/$Co_{0.4}$-MIL-53	1.0 M KOH	219	54	26
ZIF-67-350	1.0 M KOH	286	84	27
ZIF-L@Fe_{28}	1.0 M KOH	312	78	28
ZIF-8	1.0 M KOH	380	189	Present work
ZCFO-1	1.0 M KOH	330	84	
ZCFO-2	1.0 M KOH	350	88	
ZCFO-3	1.0 M KOH	360	114	

1. Grdeń, M., Alsabet, M., & Jerkiewicz, G. (2012). Surface science and electrochemical analysis of nickel foams. *ACS Applied Materials and Interfaces*, *4*(6), 3012–3021. https://doi.org/10.1021/am300380m.
2. McCrory, C. C. L., Jung, S., Peters, J. C., & Jaramillo, T. F. (2013). Benchmarking heterogeneous electrocatalysts for the oxygen evolution reaction. *Journal of the American Chemical Society*, *135*(45), 16977–16987. https://doi.org/10.1021/ja407115p.
3. A. Samadi-Maybodi, S. Ghasemi, H. Ghaffari-Rad, Application of nano-sized nanoporous zinc 2-methylimidazole metal-organic framework for electrocatalytic oxidation of methanol in alkaline solution, J. Power Sources 303 (2016) 379–387.
4. F. Asadi, S.N. Azizi, S. Ghasemi, A novel non-precious catalyst containing transition metal in nanoporous cobalt based metal-organic framework (ZIF-67) for electrooxidation of methanol, J. Electroanal. Chem. 847 (2019), 113181.
5. Y. Wang, C. Liu, J. Xiang, L. Xing, X. Ou, S. Chen, X. Xue, F. Yu, R. Li, Electrocatalytic oxidation of methanol on nickel doped metalorganic frameworks MIL-110 modified glassy

carbon electrode in alkaline medium, Int. J. Electrochem. Sci. 14 (2016) 5247–5258.

6. N. Wang, S. Liang, L. Zhang, P. Cao, L. Xu, M. Lin, Ionic liquid supported nickel-based metal-organic framework for electrochemical sensing of hydrogen peroxide and electrocatalytic oxidation of methanol, Colloids Surf. A 603 (2020), 125199.
7. S.J. Hoseini, M. Bahrami, S.M. Nabavizadeh, ZIF-8 nanoparticles thin film at an oil-water interface as an electrocatalyst for the methanol oxidation reaction without the application of noble metals, New J. Chem. 43 (2019) 15811–15822.
8. Y. Liu, B. Hu, S. Wu, M. Wang, Z. Zhang, B. Cui, L. He, M. Du, Hierarchical nanocomposite electrocatalyst of bimetallic zeolitic imidazolate framework and MoS_2 sheets for non-Pt methanol oxidation and water splitting, Appl. Catal. B Environ. 258 (2019), 117970.
9. A.P., B. Habibi, Nickel ions incorporated zinc-mesoporous metal organic frameworks thin films nanocomposite modified glassy carbon electrode for electrocatalytic oxidation of methanol in alkaline media, New J. Chem. 45 (2021) 2597–2608.
10. L. Yaqoob, T. Noor, N. Iqbal, H. Nasir, N. Zaman, Development of nickel-BTC-MOF-derived nanocomposites with rGO towards electrocatalytic oxidation of methanol and its product analysis, Catalysts 9 (2019) 856.
11. T.V.M. Sreekanth, N. D. Nam, J. Kim, K. Yoo, SnO_2 QDs@$CoFe_2O_4$ NPs as an efficient electrocatalyst for methanol oxidation and oxygen evolution reactions in alkaline media, Journal of Electroanalytical Chemistry, 2020, 873, 114363.
12. S. Zhu, J. Lei, Y. Qin, L. Zhang, L. Lu, Spinel oxide $CoFe_2O_4$ grown on Ni foam as an efficient electrocatalyst for oxygen evolution reaction, RSC Advances, 2019, 9, 13269-13274.
13. S. Bi, J. Li, Q. Zhong, C. Chen, Q. Zhang, Y. Yao, Low-cost $CoFe_2O_4$/biomass carbon hybrid from metal-enriched sulfate reducing bacteria as an electrocatalyst for water oxidation, RSC Adv., 2018, 8, 22799.
14. Y. Ding, J. Zhao, W. Zhang, J. Zhang, X. Chen, F. Yang, X. Zhang, Single-Walled Carbon Nanotubes Wrapped $CoFe_2O_4$ Nanorods with Enriched Oxygen Vacancies for Efficient Overall Water Splitting, ACS Appl. Energy Mater. 2019, 2, 1026-1032.
15. G. Zhu, X. Li, Y. Liu, W. Zhu, X. Shen, Activating CoFe2O4 electrocatalysts by trace Au for enhanced oxygen evolution activity, Applied Surface Science., 2019, 478, 206-212.
16. C. Mahala, M. D. Sharma, M. Basu, 2D nanostructures of $CoFe_2O_4$ and $NiFe_2O_4$: efficient

oxygen evolution catalyst, Electrochimica Acta, 2018, 273, 462-473.

17. J. Geng, L. Kuai, E. Kan, Q. Wang, B. Geng, Precious-Metal-Free Co–Fe–O/rGO Synergetic Electrocatalysts for Oxygen Evolution Reaction by a Facile Hydrothermal Route, ChemSusChem, 2015, 8, 659-664.
18. K-L. Yan, X. Shang, Z-Z Liu, B. Dong, S-S. Lu, J-Q Chi, W-K Gao, Y-M. Chai, C-G Liu, A facile method for reduced $CoFe_2O_4$ nanosheets with rich oxygen vacancies for efficient oxygen evolution reaction, International Journal of Hydrogen Energy, 2017, 42, 24150-24158.
19. M. Sun, D. Lin, S. Wang, T. Zhang, D. Wang, J. Li, Facile Synthesis of $CoFe_2O_4$-CoFex/C Nanofibers Electrocatalyst for the Oxygen Evolution Reaction, Journal of The Electrochemical Society, 166 (10) H412-H417 (2019).
20. Q. Y. Li, L. Zhang, Y. X. Xu, Q. Li, H. Xue and H. Pang, ACS Sustain. Chem. Eng., 2019, 7, 5027–5033.
21. H. Wang, F.-X. Yin, B.-H. Chen, X.-B. He, P.-L. Lv, C.-Y. Ye and D.-J. Liu, Appl. Catal. B Environ., 2017, 205, 55–67.
22. S. Dou, C.-L. Dong, Z. Hu, Y.-C. Huang, J. Chen, L. Tao, D. Yan, D. Chen, S. Shen, S. Chou and S. Wang, Adv. Funct. Mater., 2017, 27, 1702546.
23. S. Wang, Y. Hou, S. Lin and X. Wang, Nanoscale, 2014, 6, 9930.
24. Y Wang, Y Wang, Li Zhang, et al., Inorg. Chem. Front. 6 (2019) 2514-2520.
25. V.K. Abdelkader-Fernández, D.M. Fernandes, S.S. Balula, et al., J. Mater. Chem. A. 8 (2020) 13509-13521.
26. F. L Li, Q. Shao, X Huang, et al., Angew. Chem. Int. Ed. 57 (2018) 1888-1892.
27. R. M Zhu, J. W Ding, J. P Yang, et al., ACS Appl. Mater. Interfaces 12 (2020) 25037−25041.
28. Z. Xiao and F. Xu, A two-dimensional zeolitic imidazolate framework loaded with an acrylate-substituted oxoiron cluster as an efficient electrocatalyst for the oxygen evolution reaction, New J. Chem., 2022, 46, 11095-11100.